Relaxation effects in the photoionization time delay near the 3*s* Cooper minimum of Ar

A. Ganesan [1], S. Banerjee,[2] S. Baral [3,4], J. Jose [3,*], P. C. Deshmukh,[5,6] and S. T. Manson [7]

[1]*Department of Physics, J.B.A.S College for Women, Chennai, Tamil Nadu, India*

[2]*Center for Free-Electron Laser Science (CFEL), Deutsches Elektronen-Synchrotron DESY, Notkestr. 85, 22607 Hamburg, Germany*

[3]*Department of Physics, Indian Institute of Technology Patna, Bihta, Bihar 801103, India*

[4]*Center for Research and Exploration in Space Science and Technology, NASA/GSFC, Greenbelt, Maryland 20771, USA*

[5]*Center for Atomic, Molecular, and Optical Sciences and Technologies (CAMOST), Joint Initiative of IIT Tirupati and IISER Tirupati, Tirupati, Andhra Pradesh, India*

[6]*School of Computer Science and Engineering, RV University, Bengaluru, India*

[7]*Department of Physics and Astronomy, Georgia State University, Atlanta, Georgia 30303, USA*

(Received 15 January 2025; accepted 14 April 2025; published 2 May 2025)

The discrepancy in the attosecond time delay between theory and experiment near the 3*s* Cooper minimum (CM) of Ar is addressed. It is found that inclusion of the relaxation effects in the time delay difference between Ar 3*s* and 3*p* photoionization near the 3*s* CM dramatically alters the 3*s* time delay and brings the theory into substantial agreement with experiment using the relativistic-random-phase approximation with relaxation. The key point is that 3*s* photoionization is dominated by interchannel coupling in this region and the interchannel coupling matrix elements were found to be considerably altered by the inclusion of relaxation. This implies that relaxation should be important for any atomic or molecular transition that is dominated by interchannel coupling.

DOI: 10.1103/PhysRevA.111.052805

I. INTRODUCTION

With the advent and developments in the field of attosecond physics, photoionization time delay can now be measured [1–3]. The measurements have opened a pathway to address electron dynamics from a new perspective—the temporal domain. Although the theoretical description of the time delay was established more than half a century ago by Eisenbud [4], Wigner [5], and Smith [6], the experimental realization of the concept happened relatively recently. Subsequent studies led to detailed investigations of the effects of shape resonances [7], Cooper minima [8,9], autoionization resonances [10], two-electron ionization-plus-excitation shake-up (SU) processes [11], spin-orbit effects [12], etc., on the attosecond time delay in the photoemission process.

From the perspective of temporal delay, the noble gas atoms attracted considerable attention because they are monoatomic gases and, thus, relatively easy to work with experimentally; among them, argon has been particularly widely studied. Photoionization studies of the inner and outer subshells of atomic argon have been extensively reported in the literature [13–18]. In addition, photoionization cross sections, angular distribution asymmetry parameter, branching ratios, phase of the matrix elements, and the photoionization Wigner time delay for argon have been reported using different theoretical techniques [14,19–23]. From the experimental perspective, using interferometric techniques, the attosecond time delay difference in the photoemission from the 3*s* and 3*p* subshells of argon has been measured [3,24,25]. In particular, close to the 3*s* ionization Cooper minimum (CM), where strong interchannel coupling effects are prominent, the time delay has been scrutinized experimentally [24], and further experimental efforts confirmed this result, which differed significantly from theoretical predictions. This underscored the need for the inclusion of additional physical effects in the photoionization calculation of argon to satisfactorily explain the attosecond time delay difference between 3*s* and 3*p* photoemission [26].

From a theoretical perspective, there have been numerous attempts to calculate the photoionization time delay in argon [27,28]. This increased interest in the photoionization time delay difference of the 3*s* and 3*p* subshells is due in part to the significance of the correlation effects, specifically near the 3*s* CM region. It is well known that within an approximation like Hartree-Fock, which does not include the Coulomb correlations, the 3*s* ionization channel does not possess a CM in the continuum [14]; it is manifested only when interchannel coupling with the 3*p* photoionization channels is included in the calculation [29].

Most of the sophisticated theoretical methods agreed with the delay difference in 3*s*-3*p* photoionization in the 3*p* CM region [25]. Nevertheless, after several attempts employing various theoretical techniques, the qualitative and quantitative accuracy of $\tau_{3s\text{-}3p}$ with the experiment was missing in the region of 3*s* CM, and the discrepancy continued as a conundrum. It is very evident from several studies [22–25,27,30,31] with different theoretical approaches that the time delay near the 3*s* CM in argon is significantly influenced by the electron correlation; however, predicting the correct trend for the phase and delay remained an open question. Results based on the time-dependent local density approximation (TDLDA) approach predict a negative delay for $\tau_{3s\text{-}3p}$ over the whole 3*s* CM region, whereas the other approaches suggest a gradual

*Contact author: jobin.jose@iitp.ac.in

rise to a large positive value in the same energy region. Experiments in the past [2,24], along with a recent one [25], support the former trend. A new experiment, as yet unpublished, also shows the negative time delay in the $\tau_{3s\text{-}3p}$ around the $3s$ Cooper minimum region [32], which supports the existing experimental data.

A recent work [25] has reported experimental results of the atomic delay difference between the $3s$ and $3p$ subshells of argon in the region of $3s$ (38–45 eV) and $3p$ (45–60 eV) CM. A discrepancy between the experimental data and the theory calculated using what they call a 2P2C relativistic-random-phase approximation with exchange (RPAE) technique [25] is observed to be more significant in the region of the $3s$ CM when compared to the region of the $3p$ CM. However, a suggestive calculation indicated that the emission of electron channels from strong shake-up (SU) processes could likely be the reason for the unsatisfactory agreement [25]. Another recent theoretical investigation also suggested the possible importance of the inclusion of the SU channels [33].

In the present work, it is suggested that the discrepancy between theory and experiment is primarily due to core relaxation of the target ion resulting from the photoemission process. It has long been well known that such relaxation affects the calculated photoionization results at all levels of approximation, from the simple Hartree-Fock (HF) [14] to the much more sophisticated approaches that include significant correlation such as the relativistic-random-phase approximation (RRPA) [15]. Recently, however, it has been found in a rather different context that relaxation effects are particularly significant for processes where interchannel coupling is important [34]. Thus, since the very existence of the $3s$ CM is the result of interchannel coupling, it is likely that relaxation is important here. Accordingly, the present work aims to calculate the photoionization time delay in this energy range of argon including relaxation effects using RRPA with relaxation (RRPA-R) [35], and contrasting RRPA and RRPA-R can spotlight the effects of relaxation. Among other things, relaxation causes a redistribution of the oscillator strength in the continuum, changing it, especially near the threshold, thereby affecting the photoelectron energy of the CM in the case of Ar [36]. More importantly, the present investigation aims to understand the impact of relaxation on $\tau_{3s\text{-}3p}$ where, from the above discussion, it is expected that the major effect will involve the $3s$ subshell.

II. METHODOLOGY

The RRPA-R methodology, which takes core relaxation into account, represents an improvement on the RRPA formalism that keeps the initial- and final-state discrete orbitals the same. Since the details of RRPA are well known, along with the nonrelativistic version, RPAE [13,37,38], the focus here shall be only on the differences between RRPA and RRPA-R. Both RRPA-R and RRPA start with orbitals for the initial state of the photoionization process, resulting from a Dirac-Hartree-Fock (DHF) calculation for the initial-state N-electron system. The RRPA-R, however, uses discrete orbitals for the ion core that result from a DHF calculation for the N-1-electron ion core, i.e., relaxed orbitals, as opposed to RRPA that uses the same orbitals as in the initial state—unrelaxed

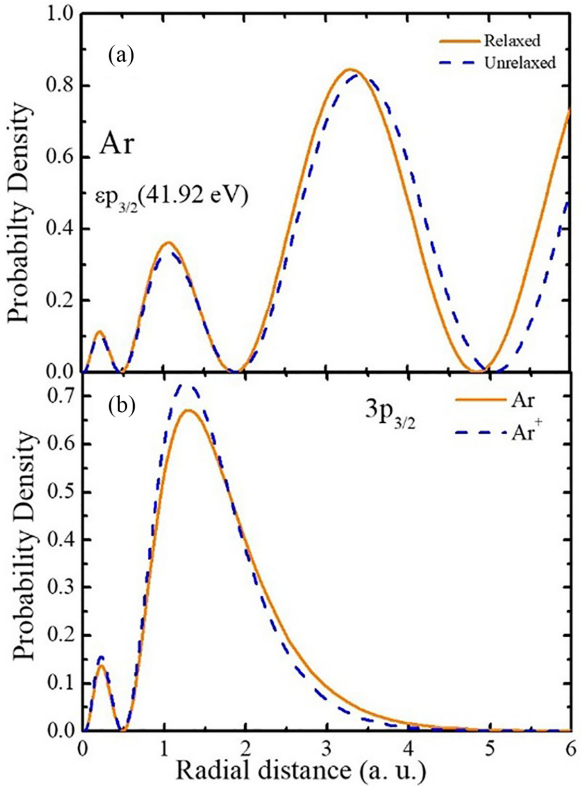

FIG. 1. Probability density plotted with radial distance for (a) $\varepsilon p_{3/2}$ from $3s$ photoionization in DHF methodology and (b) bound $3p_{3/2}$ wave function for neutral Ar and Ar^+ (where a hole is present in the $3s$ subshell).

orbitals. As an example, Fig. 1 shows the bound state $3p_{3/2}$ probability density in the final ionic Ar^+ that the $3s$ photoelectron "sees" in the RRPA and RRPA-R calculations; the atomic $3p_{3/2}$ orbital in the RRPA case and the relaxed ionic $3p_{3/2}$ for RRPA-R is shown in the lower panel. The relaxed charge density is seen to be shifted somewhat towards the nucleus owing to the relaxation. In addition, Fig. 1 also shows the final continuum orbital of the $3s$ photoionization process, $\varepsilon p_{3/2}$, calculated in a single-channel DHF approach using relaxed and unrelaxed bound orbitals, where it is evident that relaxation shifts the continuum orbital towards the nucleus.

The continuum wave functions for the photoelectron are, thus, calculated in the field of the relaxed orbitals in the RRPA-R method. This takes into account the fact that, due to the creation of the hole, the N-1 electrons rearrange themselves, thereby changing the potential of the ionic core that acts on the emerging photoelectron. Thus, two sets of bound-state orbitals are employed in the RRPA-R method to determine the photoionization dipole matrix elements [39]: the unrelaxed set of orbitals for the N-electron initial state and the set of relaxed orbitals, obtained in the presence of a hole in the photoionized subshell, for the N-1-electron final state ion core. Furthermore, the interchannel coupling matrix elements are determined using these modified continuum wave functions and relaxed discrete orbitals in the RRPA-R.

The ionization thresholds in the RRPA-R methodology are obtained from the difference between the total energies

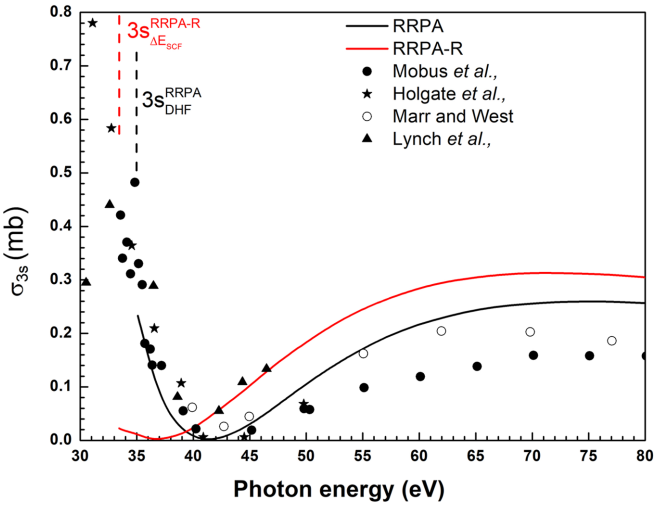

FIG. 2. Photoionization cross section of the argon $3s$ subshell. Black line: RRPA (DHF threshold). Red line: RRPA-R ($\Delta E_{\rm SCF}$ threshold). Experimental plot: open circles: Marr and West [40]; solid dots: Möbus *et al.* [41]; open triangles: Lynch *et al.* [42]; solid squares: Houlgate *et al.* [19].

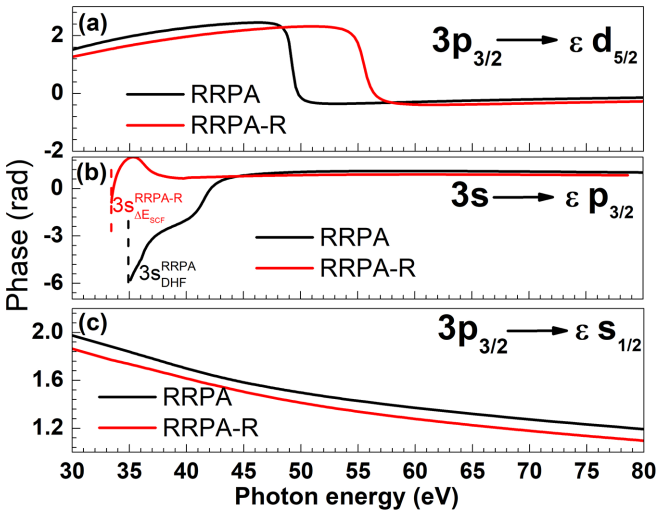

FIG. 3. Relativistic phases of the (a) $3p_{3/2} \rightarrow \varepsilon d_{5/2}$, (b) $3s \rightarrow \varepsilon p_{3/2}$, and (c) $3p_{3/2} \rightarrow \varepsilon s_{1/2}$ matrix elements in RRPA (DHF threshold) and RRPA-R ($\Delta E_{\rm SCF}$ threshold).

obtained self-consistently for the unrelaxed ground state of the N-electron atom, and the relaxed ion with a hole, respectively ($\Delta E_{\rm SCF}$ energies). A separate calculation is required to obtain the ionization threshold energy for each channel, and the Oxford-MCDF package [38] was used to obtain these energies; RRPA uses DHF energies. The $3s$ DHF and $\Delta E_{\rm SCF}$ energies are respectively 34.92 and 33.42 eV.

The use of the relaxed core potential removes the gauge invariance between the length and velocity forms of the dipole matrix elements that exist in the RRPA. This is not a critical problem since our length and velocity results are quite similar, certainly within about 10% and generally significantly better.

III. RESULTS AND DISCUSSION

The $3s$ photoionization cross section, obtained using the RRPA and the RRPA-R methods, is shown in Fig. 2. Basically, the addition of relaxation moves the cross section to lower energy by a few eV. In both cases, the CM lies a few eV above the respective thresholds. The deviation from the experiment in the RRPA-R is primarily due to the usage of different thresholds in both calculations; the usage of different thresholds is responsible for the shift in the CM. Additionally, the consideration of instantaneous relaxation overestimates further.

Since the time delay is essentially the energy derivative of the phase of the photoionization matrix element, it is of interest to look at these phases. When the matrix element exhibits a CM, the phase of the complex matrix element also changes by about π radians [8,9]. The phase of the $3p_{3/2} \rightarrow \varepsilon d_{5/2}$ transition for the RRPA and RRPA-R calculations is shown in Fig. 3(a) where it is seen that, in both calculations, there is a change of phase by about π radians around the CM. The relaxation shifts the CM by about 5 eV; aside from this shift, the phases are qualitatively the same. A similar shift occurs for the $3p_{3/2} \rightarrow \varepsilon d_{3/2}$ and the $3p_{1/2} \rightarrow \varepsilon d_{3/2}$ transitions as well. This is rather expected behavior as the shifts of the wave functions, as seen in Fig. 1, are relatively small. Looking at the $3s \rightarrow \varepsilon p_{3/2}$ phase in Fig. 3(b), it is seen that the relaxation renders the RRPA-R phase qualitatively completely different from the unrelaxed RRPA phase. Both phases exhibit a change of π radians around the CM but the details are decidedly different. One may anticipate corresponding qualitative changes in the time delay due to the relaxation effects in these transitions. It is likewise interesting to see the effect of relaxation on the phase and the time delay of the $3p_j \rightarrow \varepsilon s_{1/2}$ transition as it dominates over the $3p_j \rightarrow \varepsilon d$ channels at the CM. Figure 3(c) shows that the phase of the $3p_{3/2} \rightarrow \varepsilon s_{1/2}$ transition decreases gradually at the CM of other channels and the effect due to relaxation is not significant, as for the time delay.

The time delays of individual channels resulting from the present calculations are shown in Fig. 4(a). Owing to the dramatic difference in $3s$ transition phases with and without relaxation, the resulting $3s$ time delays are also strikingly different, while the $3p$ time delay is merely shifted by the energy shift in the corresponding phase. Further, the time delay differences along with experimental results are plotted in Fig. 4(b). The $3s$-$3p$ time delay difference, $\tau^{w}_{3s\text{-}3p}$, from the RRPA-R calculation is completely different from the RRPA result in the $3s$ CM region; τ^{w}_{i-j} stands for the Wigner time delay difference in the transition from subshells i and j. The RRPA result shows a rather large $3s$ time delay in the $3s$ CM region, while the RRPA-R time delay is negative in the same region. More importantly, the relaxation brings theory into reasonably good agreement with experiment, as seen in Fig. 4. Not only is the time delay difference inverted, but also the minimum is displaced in energy, so that the agreement with the experiment is better.

Using the framework presented in the electron interferometry technique [25], one can get direct access to $\tau^{A}_{3s\text{-}3p} \approx \tau^{w}_{3s\text{-}3p} + \tau^{cc}_{3s\text{-}3p}$, where $\tau^{cc}_{3s\text{-}3p}$ is the measurement-induced time delay difference due to the electrons being probed by the laser field in long-range Coulombic potential. Employing the

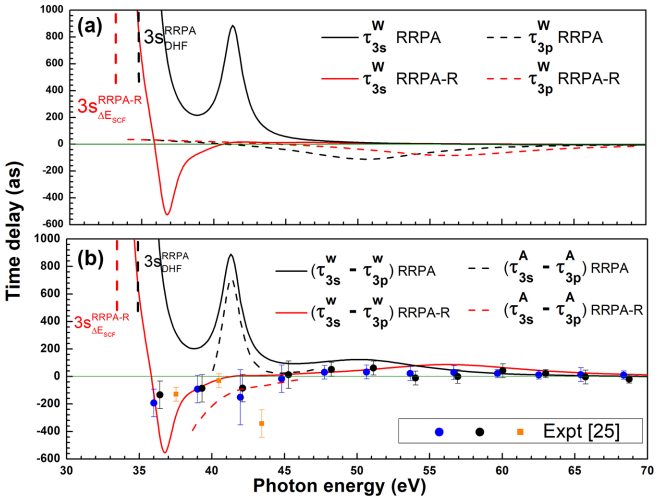

FIG. 4. Photoionization time delay of argon: (a) $3s$ and $3p$ subshells in RRPA (DHF threshold) and RRPA-R (ΔE_{SCF} threshold); (b) the time delay difference. The experiments reported in Ref. [25] were performed independently at the ATTO Lab facility in Saclay, France (blue dots for sidebands and orange squares for harmonics), and at Lund University, Sweden (black dots).

estimate of the universal time delay for $\tau^{cc}_{3s\text{-}3p}$ [3], the experimentally measurable $\tau^{A}_{3s\text{-}3p}$ is approximately calculated and presented (dash-dot-dot line) in a limited range in Fig. 4(b). One can notice that the trend of $\tau^{A}_{3s\text{-}3p}$ is unchanged even after adding $\tau^{cc}_{3s\text{-}3p}$, still rendering a good agreement between RRPA-R and the experiment.

The question now is why relaxation has such a profound qualitative effect upon the $3s$ time delay but only a small quantitative effect on $3p$. As mentioned earlier, interchannel coupling plays a crucial role in $3s$ photoionization near the CM, but the same is not true in the $3p$ case [15]. To understand how interchannel coupling works in detail, and why the effects of interchannel coupling are so complicated, we look at the problem from a perturbation theory point of view. The fully coupled (correlated) dipole matrix element, $D_i(E)$, of channel i can be written in terms of the uncoupled (single-particle) matrix elements, $M_j(E)$, of the various photoionization channels j as [43]

$$D_i(E) = M_i(E) + \sum_j \int dE' \frac{\langle \psi_i(E)|H - H_0|\psi_j(E')\rangle}{E - E'} \times M_j(E'), \tag{1}$$

where $H - H_0$ is the perturbing Hamiltonian, and $\psi_i(E)$ and $\psi_j(E')$ are, respectively, the unperturbed (uncoupled single-particle) final continuum state wave functions of channels i and j with energies E and E'; the second term on the right side represents the interchannel coupling contribution to the dipole matrix element. Clearly, this shows that the interchannel contribution of a given channel j depends upon the magnitude and sign of its dipole matrix element, $M_j(E')$, the interchannel coupling matrix element, $\langle \psi_i(E)|H - H_0|\psi_j(E')\rangle$, and whether or not channel j is open (energetically allowed) or closed at the given energy. But most importantly, the influence of the interchannel coupling term is generally largest when channel j can occur at the same energy as channel i, i.e., they are degenerate so the denominator can vanish. It is also evident that, at a given energy E, when a channel j with dipole matrix element $M_j(E)$ is significantly larger than the unperturbed matrix element $M_i(E)$ in channel i, it is likely that the second term, the interchannel coupling term, will dominate. In other words, when a strong (large dipole matrix element) channel is degenerate with a weak one, there is the likelihood of the matrix element of the weak channel being significantly altered by the interchannel coupling with the strong one [44].

A separate independent particle calculation on a DHF level (not shown) makes it clear that the relaxation alone causes only quantitative differences in the single-particle $3p$ and $3s$ matrix elements, the $M_i(E)$ of the above equation. Furthermore, since the $3p$ matrix elements (cross sections) dominate this energy region, the second (interchannel coupling) term in the equation is relatively unimportant for the Ar $3p$ channels, thereby leading to the observed phenomenology—just a small quantitative change resulting from relaxation. On the other hand, as mentioned earlier, the weaker $3s$ channels are dramatically modified by the stronger $3p$ channels, i.e., the $3s$ dipole matrix elements are dominated by interchannel coupling—the second term in the equation. This suggests that the important effect of relaxation is not in the dipole matrix elements directly, but rather in the effects upon the interchannel coupling matrix elements. Thus, it follows that the interchannel coupling is always present; we can get significant relaxation-induced qualitative changes only when the interchannel coupling dominates (like it does for the Ar $3s$ photoionization). Therefore, the Ar photoionization is a classic example, which showcases qualitative changes in the time delay due to the relaxation effects. This is entirely in keeping with the earlier observation of the importance of the relation to interchannel coupling in an entirely different context [34].

Despite the qualitative agreement, there exists a slight quantitative mismatch between the RRPA-R and the experiment. This might be due to the omission of the SU channels, which could alter the results somewhat, as suggested earlier [25,33]. While some of these effects cancel out in the time delay *difference*, there still could be some effects.

IV. CONCLUSIONS

In summary, we have demonstrated that the relaxation of atomic orbitals strongly affects the interchannel coupling matrix element and, as a result, has a considerable effect on the attosecond time delay for Ar $3s$ photoionization, which is dominated by interchannel coupling; inclusion of the relaxation has brought theory into substantial agreement with experiment in the region of the $3s$ CM and resolved a long-standing difficulty.

Of importance is that the implications of these results should be quite general. There likely will be significant effects of relaxation for any transition that is dominated by interchannel coupling, and such processes abound in Atomic, Molecular and Optical (AMO) physics [45].

ACKNOWLEDGMENTS

We thank Anne L'Hullier for a critical reading of the manuscript. The work of J.J. was supported by the ANRF, India through project CRG/2022/000191. The work of S.T.M. was supported by the U.S. Department of Energy, Office of Basic Sciences, Division of Chemical Science, Geosciences and Biosciences under Grant No. DE-SC0025316. Calculations by A.G. were carried out on Aqua cluster of IITM, Chennai.

DATA AVAILABILITY

The data that support the findings of this article are not publicly available. The data are available from the authors upon reasonable request.

[1] P. C. Deshmukh, S. Banerjee, and S. T. Manson, Can. J. Phys, **103**, 1 (2025).
[2] M. Schultze *et al.*, Science **328**, 1658 (2010).
[3] K. Klunder, J. M. Dahlström, M. Gisselbrecht, T. Fordell, M. Swoboda, D. Guénot, P. Johnsson, J. Caillat, J. Mauritsson, A. Maquet, R. Taïeb, and A. L'Huillier, Phys. Rev. Lett. **106**, 143002 (2011).
[4] L. Eisenbud, The formal properties of nuclear collisions, Ph.D. thesis, Princeton University, 1948.
[5] E. P. Wigner, Phys. Rev. **98**, 145 (1955).
[6] F. T. Smith, Phys. Rev. **118**, 349 (1960).
[7] J. L. Dehmer, J. Chem. Phys. **56**, 4496 (1972).
[8] J. W. Cooper, Phys. Rev. **128**, 681 (1962).
[9] J. W. Cooper, Phys. Rev. Lett. **13**, 762 (1964).
[10] C. Cirelli, C. Marante, S. Heuser, C. L. M. Petersson, Á. J. Galán, L. Argenti, S. Zhong, D. Busto, M. Isinger, S. Nandi, and S. Maclot, Nat. Commun. **9**, 955 (2018).
[11] M. Isinger, R. J. Squibb, D. Busto, S. Zhong, A. Harth, D. Kroon, S. Nandi, C. L. Arnold, M. Miranda, J. M. Dahlström, and E. Lindroth, Science **358**, 893 (2017).
[12] I. Jordan, M. Huppert, S. Pabst, A. S. Kheifets, D. Baykusheva, and H. J. Wörner, Phys. Rev. A **95**, 013404 (2017).
[13] M. Ya. Amusia, N. A Cherepkov, and L. V. Chernysheva, Zh. Eksp. Teor. Fiz. **60**, 160 (1971) [Sov. Phys. JETP **33**, 90 (1971)].
[14] D. J. Kennedy and S. T. Manson, Phys. Rev. A **5**, 227 (1972).
[15] W. R. Johnson and K. T. Cheng, Phys. Rev. A **20**, 978 (1979).
[16] J. Berkowitz, *Photoabsorption, Photoionization, and Photoelectron Spectroscopy* (Academic, New York, 1979).
[17] K. N. Huang, W. R. Johnson, and K. T. Cheng, At. Data Nucl. Data Tables **26**, 33 (1981).
[18] A. F. Starace, in *Handbuch der Physik*, edited by W. Mehlhorn (Springer, Berlin, 1982), Vol. 31, pp. 1–121.
[19] R. G. Houlgate, K. Codling, G. V. Marr, and J. B. West, J. Phys. B **7**, L470 (1974).
[20] M. Kutzner, Q. Shamblin, S. E. Vance, and D. Winn, Phy. Rev. A **55**, 248 (1997).
[21] A. Kheifets, A. Mandal, P. C. Deshmukh, V. K. Dolmatov, D. A. Keating, and S. T. Manson, Phys. Rev. A **94**, 013423 (2016).
[22] S. Saha, A. Mandal, J. Jose, H. R. Varma, P. C. Deshmukh, A. S. Kheifets, V. K. Dolmatov, and S. T. Manson, Phys. Rev. A **90**, 053406 (2014).
[23] J. M. Dahlström, T. Carette, and E. Lindroth, Phys. Rev. A **86**, 061402(R) (2012).
[24] D. Guénot *et al.*, Phys. Rev. A **85**, 053424 (2012).
[25] C. Alexandridi *et al.*, Phys. Rev. Res. **3**, L012012 (2021).
[26] D. Guénot *et al.*, J. Phys. B **47**, 245602 (2014).
[27] M. Magrakvelidze, Mohamed El-Amine Madjet, G. Dixit, M. Ivanov, and H. S. Chakraborty, Phys. Rev. A **91**, 063415 (2015).
[28] A. S. Kheifets, Phys. Rev. A **87**, 063404 (2013).
[29] M. Ya Amusia, V. K. Ivanov, N. A. Cherepkov, and L. V. Chernysheva, Phys. Lett. A **40**, 361 (1972).
[30] L. W. Pi and A. S. Landsman, Appl. Sci. **8**, 322 (2018).
[31] J. Vinbladh, J. M. Dahlström, and E. Lindroth, Phys. Rev. A **100**, 043424 (2019).
[32] S. Liu and A. L'Huillier (private communication).
[33] Jia-Bao Ji, A. S. Kheifets, M. Han, K. Ueda, and H. J. Wörner, New J. Phys. **26**, 093014 (2024).
[34] K. P. R. V. Silva, C. R. Munasinghe, and S. T. Manson, in *Proceedings of the Young Scientists' Conference on Multidisciplinary Research-2024* (Young Scientists' Association, National Institute of Fundamental Studies, Sri Lanka, 2024).
[35] V. Radojević, M. Kutzner, and H. P. Kelly, Phys. Rev. A **40**, 727 (1989).
[36] J. Jose, G. B. Pradhan, V. Radojević, S. T. Manson, and P. C. Deshmukh, J. Phys. B **44**, 195008 (2011).
[37] M. Ya. Amusia, *Atomic Photoeffect* (Plenum, New York, 1990).
[38] I. P. Grant, B. J. McKenzie, P. H. Norrington, D. F. Mayers, and N. C. Pyper, Comput. Phys. Commun. **21**, 207 (1980).
[39] S. T. Manson and A. F. Starace, Rev. Mod. Phys. **54**, 389 (1982).
[40] G. V. Marr and J. B. West, At. Data Nucl. Data Tables **18**, 497 (1976).
[41] B. Möbus, B. Magel, K. H. Schartner, B. Langer, U. Becker, M. Wildberger, and H. Schmoranzer, Phys. Rev. A **47**, 3888 (1993).
[42] M. J. Lynch, A. B. Gardner, K. Godling, and G. V. Marr, Phys. Lett. A **43**, 237 (1973).
[43] U. Fano, Phys. Rev. **124**, 1866 (1961).
[44] E. W. B. Dias *et al.*, Phys. Rev. Lett. **78**, 4553 (1997).
[45] S. T. Manson, Can. J. Phys. **103**, 21 (2025).